## Original Article
# Synergistic effects of *Lactobacillus rhamnosus* culture supernatant and bone marrow mesenchymal stem cells on the development of alcoholic steatohepatitis in mice

Chao Cai[1*], Da-Zhi Chen[2*], Li-Chao Ge[1], Wen-Kai Chen[1], Sha-Sha Ye[1], Wei-Wei Ye[1,3], Ying Tao[1], Rui Wang[1], Ji Li[1], Zhuo Lin[1], Xiao-Dong Wang[1], Lan-Man Xu[1,4,5], Yong-Ping Chen[1]

[1]Department of Infectious Diseases, The First Affiliated Hospital of Wenzhou Medical University, Hepatology Institute of Wenzhou Medical University, Wenzhou Key Laboratory of Hepatology, Wenzhou 325000, Zhejiang, China; [2]Department of Gastroenterology, The First Hospital of Peking University, Beijing, China; [3]The Affiliated Yiwu Central Hospital of Wenzhou Medical University, Wenzhou, Zhejiang, China; [4]Department of Infectious Diseases and Liver Diseases, Ningbo Medical Center Lihuili Eastern Hospital, Ningbo 315040, Zhejiang, China; [5]Department of Infectious Diseases and Liver Diseases, Taipei Medical University Ningbo Medical Center, Ningbo 315040, Zhejiang, China. *Equal contributors.

**Abstract:** The gut microbiota has been shown to play an important role in chronic liver disease. It has been found that both *Lactobacillus rhamnosus* and its culture supernatant have the potential to mitigate alcoholic steatohepatitis. However, the exact mechanism is still not fully understood. Bone marrow mesenchymal stem cells have immunosuppressive effects with few side effects. The synergistic effect between *Lactobacillus rhamnosus* culture supernatant and bone marrow mesenchymal stem cells (BMMSCs) deserves further observation. In this study, a mouse model of chronic alcoholic hepatitis was established by eight weeks of Lieber-DeCarli liquid diet feeding; and LGG-s, BMMSCs or a combination of the two were used to explore a new therapeutic method for alcoholic liver disease and to study the mechanism. The results showed that the combined LGG-s and BMMSC treatment might have a synergistic effect and could improve the symptoms of alcoholic hepatitis by regulating inflammation, autophagy and lymphocyte subsets through the PI3k/NF-kB and PI3K/mTOR pathways. With the treatment, the autophagy rate accelerated, and alcohol-induced natural killer B (NKB) cell and follicular helper T (TFH) cell numbers decreased. These findings suggest that the development of alcoholic hepatitis may occur via PI3K/NF-kB and PI3K/mTOR pathway overactivation as well as through NKB and TFH cell imbalances. Moreover, LGG-s and BMMSCs can regulate these factors and alleviate the disease.

**Keywords:** Gut microbiota, mTOR, bone marrow mesenchymal stem cells, alcoholic liver disease, natural killer-like B cells

## Introduction

With a gradual and steady decrease in viral hepatitis B infections due to the use of the hepatitis B vaccine as well as the improvement of living conditions, fatty liver diseases, especially steatohepatitis, have steadily increased in recent decades and become a primary issue to the health of the liver [1]. In both alcoholic and nonalcoholic fatty liver disease, fatty liver progresses from steatosis, steatohepatitis, cirrhosis to hepatocellular carcinoma [2]. Steatohepatitis is an inflammatory condition in the liver, and investigation of steatohepatitis has revealed that lipid peroxidation and local inflammatory cytokines released by the accumulation of fat in liver cells are the major causes of liver fibrosis and cirrhosis [3].

Inflammation is a complex biological response that involves cytokines, immune cells and blood vessels. Although several cytokines are important in inflammation, NF-kB is one of the most inflammation-inducible factors in nonalcoholic fatty liver disease [4, 5], and its expression is elevated in alcoholic liver disease [6]. However, NF-kB overexpression alone cannot explain the autophagy and Th17-Treg percentage imbal-

ance observed in fatty liver diseases [7-11]. Recently, the mammalian rapamycin receptor pathway has been found to be significantly activated in various inflamed tissues. Several studies have revealed that inflammation can be reduced by inhibiting the PI3K/mTOR pathway [12-15]. For example, in autoimmune hepatitis, inhibition of the PI3K/mTOR pathway reduces inflammation [16-18]. Moreover, the PI3K/mTOR pathway has been shown to be closely associated with autophagy [19]. Autophagy is a self-protective process against harmful external stimuli, similar to inflammatory processes [20].

Changes in the proportion of lymphocyte subsets play a crucial role in immune regulation [21, 22]. We previously found that changes in the proportion of Th17 and Treg cells could affect liver damage in mice with alcoholic hepatitis. By adjusting this ratio, the alcohol-induced damage to the liver could be reduced to some extent [11]. Recently, both natural killer B cells (NKB) and follicular helper T cells (TFH) have been found to be immune adjuvant cells that have immunomodulatory effects [23-27]. Therefore, their role in the regulation of liver inflammation needs to be investigated.

Recently, gut microbiota has been found to be involved in several diseases in humans, including alcoholic fatty liver diseases [28, 29]. Dysbiosis of gut microbiota has been demonstrated to increase liver fat accumulation [30]. Moreover, fecal transplantation from patients with nonalcoholic fatty liver disease to mice treated with a high-fat diet can exacerbate liver damage [31]. Furthermore, treatment of gut microbiota to correct the dysbiosis improves clinical outcomes in a nonalcoholic disease animal model [11, 32]. Treatment of chronic-binge alcoholic model mice with LGG culture supernatant improves intestinal barrier function and the balance of Treg and TH17 cells [11]. We have previously shown that bone marrow mesenchymal stem cells and LGG-s can regulate Th17 and Treg cells, affecting the damage of alcoholic liver disease to the liver. The similar mechanisms of BMMSCs and LGG-s led us to consider whether there are direct or indirect synergistic effects between them and whether the use of both interventions can enhance the protection against liver damage caused by alcohol. According to the hypothesis above, this study aimed to explore the possible synergistic effects and the underlying mechanism.

## Material and methods

### Preparation of LGG-s

LGG was purchased from (ATCC, Rockville, MD) and cultured in MRS broth according to the manufacturer's guidelines. When the LGG density reached $10^9$ colony-forming units/ml (CFU/ml), the LGG supernatant (LGG-s) was collected by filtering through 0.22 mm filters. LGG-s was stored at 0-4°C for use.

### Animal experiments and sample collection

Wild-type (WT) male C57BL/6 mice weighing 18~20 g at six weeks of age were purchased from the Shanghai Laboratory Animal Center (Shanghai, China). Mice were fed a Lieber-DeCarli control diet for 2 weeks for adaptation to a liquid diet and then fed a different proportion of Lieber-DeCarli ethanol diet for one week starting at a ratio of the Lieber-DeCarli control diet to the Lieber-DeCarli ethanol diet (5% ethanol) of 2:1 to 1:1 and increasing to 1:2 on days 2, 4 and 6, with the exception of mice in the normal control group. At the end of the adaptation period, mice were fed a complete Lieber-DeCarli ethanol diet. There were 5 experimental groups with 6 mice in each group: group 1: normal control group (N) with Lieber-DeCarli control diet only; group 2: alcohol model group (M) with Lieber-DeCarli ethanol diet for 4 weeks; group 3: LGG-s treatment group (L) with Lieber-DeCarli ethanol diet plus LGG-s in the diet (at a dose equivalent to $10^9$ CFU/ml per mouse per day) [11, 33]; group 4: BMMSC treatment group (B) with a Lieber-DeCarli ethanol diet plus injection of BMMSCs via the tail vein once per week for a total of 3 times at the beginning of the second week, third week and fourth week; and group 5: LGG-s and BMSC treatment group (LB) with Lieber-DeCarli ethanol diet plus the combination of LGG-s and BMSC groups as described for groups 3 and 4. At the end of the 7th week, all mice were euthanized by collecting blood from the tail vein and then by cervical dislocation as outlined in **Figure 1**. Mice were treated according to the protocols reviewed and approved by the Institutional Ethics Committee of Wenzhou Medical University, which were in accordance with the Guiding Principles for the Care and Use of Laboratory Animals in China.

### Liver enzymes assay

The collected blood was centrifuged at 1500 rpm at room temperature for 10 minutes to
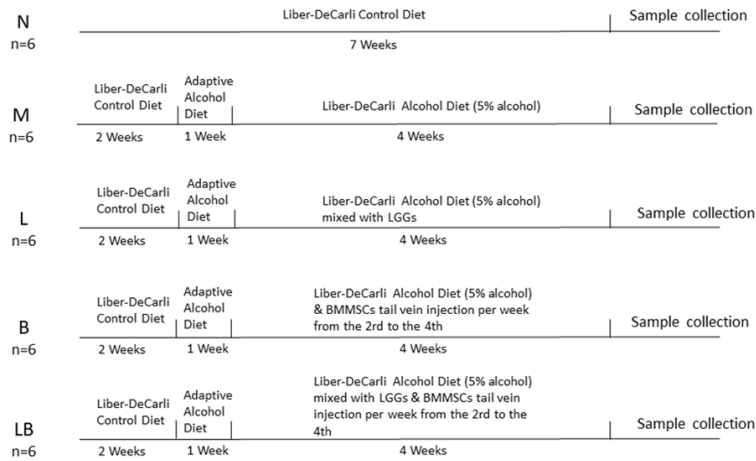
**Figure 1.** Animal treatment schedule. The experiment started with two-weeks of adaptation to liquid diet feeding with a control liquid diet followed by a one-week ethanol adaptive feeding period for all treatment groups except the control group. As shown in the figure, the total experimental time was 7 weeks.

obtain serum. Serum was then stored at -80°C until measurement. Serum ALT and AST levels were measured by an automatic biochemistry analyzer (AU5800, Beckman Coulter, USA) at the clinical biochemical laboratory of the First Affiliated Hospital of Wenzhou Medical University.

*Histochemical staining of the liver by HE and oil red O*

Paraformaldehyde (4%) was used to fix liver tissue. After fixation in paraformaldehyde and embedding in paraffin, tissue was prepared into 4-μm-thick slices and stained with hematoxylin and eosin (HE). Another part of the liver was quickly frozen after removal from mice. Frozen tissue was cut into 5-μm-thick slices and stained with oil red O in a standard protocol. Three randomly selected fields in each slide were measured with a digital image analyzer (KS400, Carl Zeiss Vision, Germany) by a technician blinded to the tissue grouping. Histological assessment was conducted by two clinical pathologists who were blind to the experiment.

*Real-time reverse transcription-polymerase chain reaction (RT-PCR) assay*

Total RNA was isolated from mouse liver tissue using an RNA isolation kit (RNAiso, Aidlab Biotechnologies Co., Beijing, China). Reverse transcriptase was conducted by a PrimeScript RT reagent kit (Takara, Otsu, Shiga, Japan). Real-time PCR was performed with a QuantStudio™ 5 Real-Time PCR System (Thermo Fisher, Waltham, MA USA) to test the expression of FOS and microRNA-29c. Expression values were compared using the delta-delta-Ct method, FOS was normalized to GAPDH and microRNA-29c was normalized to U6. RT-PCR was performed by a 7500 real-time PCR system (Applied Biosystems, Life Technologies, USA) following a PCR cycle of denaturation at 94°C for 30 seconds, annealing at 60°C for all genes for 60 seconds, and extension at 72°C for 2 minutes for 40 cycles. Primers were as follows: GAPDH: forward primer (5'->3') AAGAAGGTGGTGAAGCAGG, reverse primer (5'->3') GAAGGTGGAAGAGTGGGAGT with Tm= 60°C, raptor: forward primer (5'->3') CACGTCTTCCTTTGTCTTCACCTAC, reverse primer (5'->3') GCCTTGCCTTCTCTGACTGCTC with Tm= 60°C, rictor: forward primer (5'->3') CTCGCTTCGGCAGCACATATACT, and reverse primer (5'->3') ACGCTTCACGAATTTGCGTGTC with Tm= 60°C. Each mRNA expression value was calculated based on the expression of glyceraldehyde-3-phosphate dehydrogenase (GAPDH) as a reference gene. The final data were analyzed by the 2-ΔΔCt method.

*Western blot analysis*

Cytoplasmic protein in the liver tissue was extracted by using ice-cold RIPA solution (Biotime, Beijing, China). Twenty micrograms of the protein sample from each mouse was denatured for five minutes with 4 × gel loading buffer. After separation by 10% SDS-PAGE, proteins were transferred to a polyvinylidene fluoride membrane (Immobilon-p, Darmstadt, Germany). Membranes were blocked with 5% BSA in TBST (10 mM Tris-HCl, pH 7.5, 150 mM NaCl, 0.05% Tween-20) at 22°C for one hour and incubated with specific antibodies at 4°C for 12 hours. The membranes were then washed and incubated with a horseradish peroxidase-conjugated secondary antibody (1:5,000, Biosharp, Hefei, China) for one hour at 22°C. Protein levels were detected by chemiluminescence using an ECL kit (Thermo, Massachu-
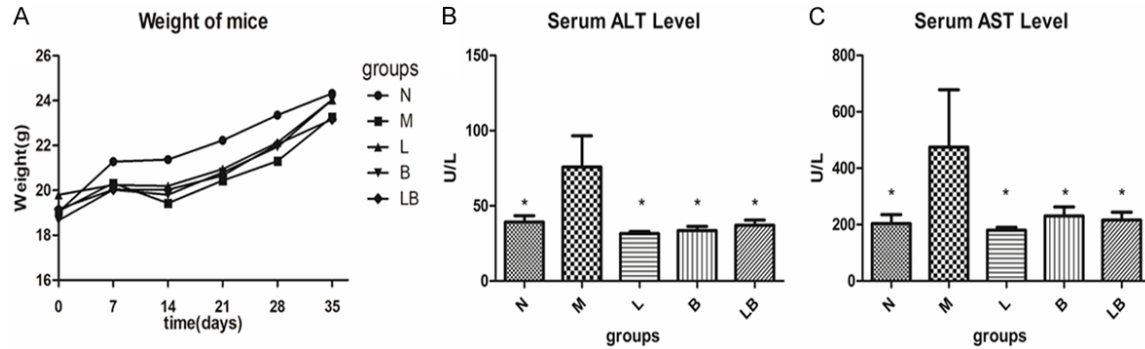
**Figure 2.** Body weight and serum aminotransferase levels. (A) Shows the body weight of mice during the treatment. (B) displays the serum ALT level in different groups, and (C) shows the serum AST level in different groups. Data are presented as the mean ± SEM from six mice in each group. *Represents P<0.05 vs group M.

setts, USA). Immunoreactive bands were digitally captured as images through a BIO-RAD ChemiDoc XRS (BIO-RAD, California, USA). The density values of the bands were measured using Image Lab (BIO-RAD, California, USA).

*Flow cytometry analysis*

Mouse spleens from different groups were removed and washed with PBS. The splenic lymphocytes were isolated by a Spleen Lymphocyte Separation kit from Multiscience (Multiscience, Hangzhou, China). After isolation of lymphocytes from the spleen, 500 μl of cell suspension solution was used to detect NKB cells and TFH cells. NKB cells were defined as $CD19^+NK1.1^+CD3^-$ B cells, and TFH cells were defined as $CD4^+CXCR5^+$ T cells. Splenic lymphocytes were incubated with fluorescently labeled CD3-FITC (eBioscience, CA, USA), CD19-APC (eBioscience) and NK1.1-PE (eBioscience), CD4-PerCP5.5 (eBioscience), and CXCR5-PE (eBioscience) monoclonal antibodies at room temperature for 30 minutes. Mouse IgG2a kappa labeled with PE (eBioscience) was used as an isotype control to avoid nonspecific binding. $CD3^-CD19^+NK1.1^+$ NKB cells and $CD4^+CXCR5^+$ FTH T cells were analyzed using the BD FACSCalibur platform (BD Bioscience, CA, USA), and the percentages of NKB cells to total B cells and TFH cells to total lymphocytes were analyzed by FlowJo software.

*Statistics*

Comparisons between multiple sets of data were performed using two-way analysis of variance (ANOVA), LSD and Dunnett's T3 tests in SPSS 20.0 software. For the cell experiments,

three independent experiments were performed for each parameter. Data are presented as the mean ± SEM. A *P* value of less than 0.05 was considered to be statistically significant.

**Results**

*LGG-s treatment, BMMSC treatment and combination treatment all have a positive effect on alcohol-induced abnormal liver function*

Body weights of mice in different groups were measured once every week. As shown in **Figure 2A**, the body weight of mice from all groups gradually increased. Although there was a gap between the body weight of control mice and body weight of mice in other groups, the difference was not statistically significant. Moreover, the body weight of mice in different groups was very close at the end of the experiment. Liver injury was assessed by aminotransferases, as indicated in **Figure 2B** and **2C**. Both serum ALT and AST levels were significantly elevated in mice fed the Lieber-DeCarli ethanol diet compared with mice fed the Lieber-DeCarli control diet. In addition, compared with the control treatment, treatment with either LGG-s, BMMSCs or a combination of LGG-s and BMMSCs significantly reduced both serum ALT and AST levels compared.

*LGG-s BMMSC combination treatment decreases liver tissue damage and liver lipid accumulation*

Liver tissue injury and lipid deposition were also examined by liver histology, as shown in **Figure 3**. There was a significant liver injury in mice fed the Lieber-DeCarli ethanol diet com-
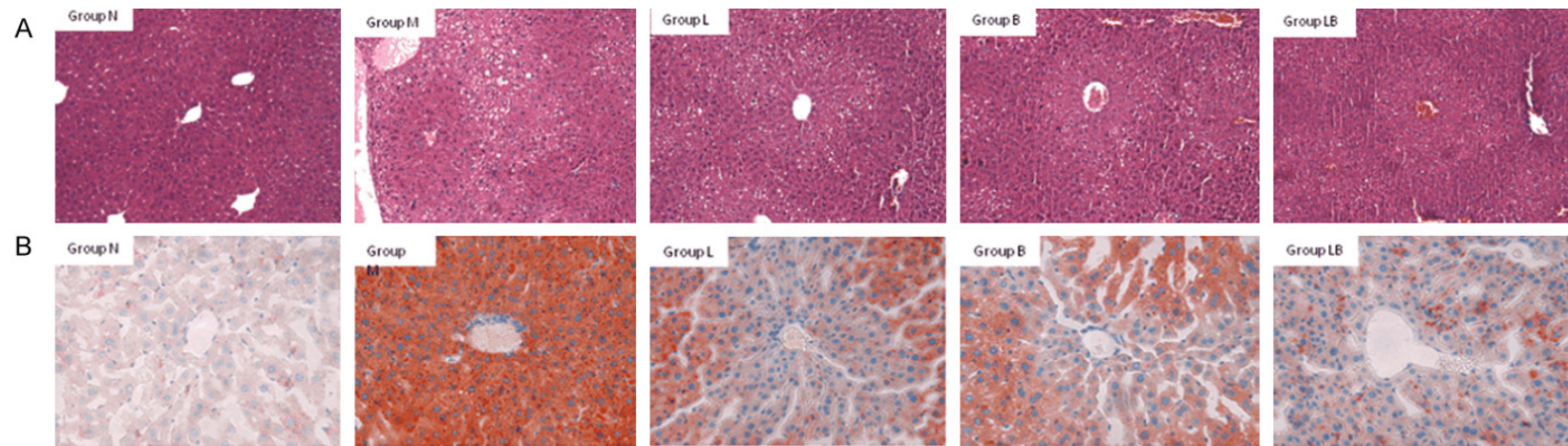
**Figure 3.** Histological examination of the livers from different groups. (A) Shows the HE staining of the livers from different groups (original magnification: ×200), and (B) displays the oil red O staining of the liver (original magnification: ×200).
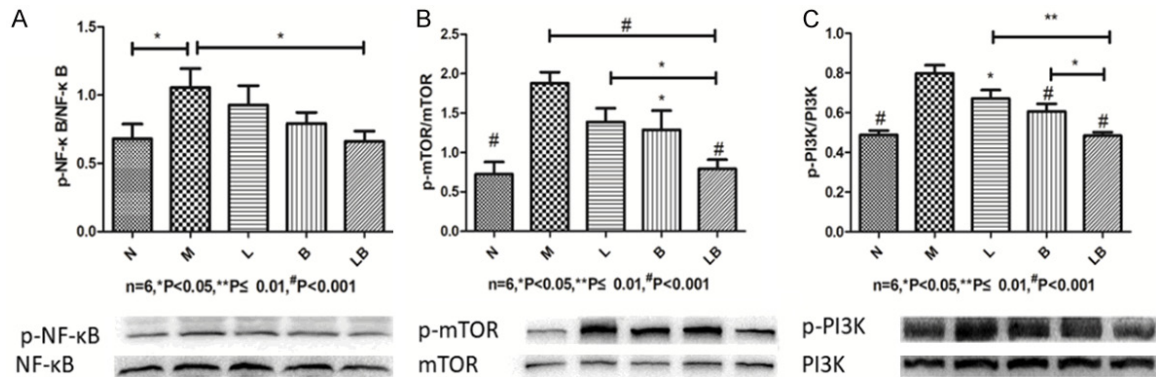
**Figure 4.** Expression of NF-kB, mTOR and PI3K in the livers from different groups. (A) Shows the results of NF-kB, (B) shows the results of mTOR, and (C) shows the results of PI3K. The upper panel is the histogram of the ratio of the phosphorylated form to the total form, and the bottom panel represents typical pictures of the Western blots. Data are presented as the mean ± SEM from six mice in each group. Symbols without a line below: *represents P<0.05, **represents P<0.01, #represents P<0.001 vs group M. Symbols with line below: *represents P<0.05, **represents P<0.01, #represents P<0.001 vs group M or LB.

pared to mice fed the Lieber-DeCarli control diet (**Figure 3A**). However, LGG-s, BMMSCs, and the combination of LGG-s and BMMSCs significantly reduced liver injury but did not completely reverse the liver injury. The lipid deposition results are shown in **Figure 3B**. Compared to mice fed the Lieber-DeCarli control diet, mice fed the Lieber-DeCarli ethanol diet showed significant lipid deposition. Moreover, all three treatment options reduced lipid deposition but did not return lipid deposition in the liver back to the level in livers of normal mice. These improvements were increased in the mice that received a combination of LGG-s and BMMSCs. In addition, there was no significant evidence of liver fibrosis as assessed by Masson's trichome staining due to the short course of ethanol intake (data not shown).

*The therapeutic effect of the combined treatment is mediated by NF-KB, PI3K, and mTOR*

The mechanism of liver injury was further investigated by examining the expression and phosphorylation of the inflammatory signaling molecules NF-kB and mTOR, as shown in **Figure 4**. There was a significant decrease in phosphorylated forms of NF-kB (**Figure 4A**), mTOR (**Figure 4B**) and PI3K (**Figure 4C**).

*The mechanism of the combined therapy may involve autophagy*

Since the PI3K/mTOR signaling pathway is also involved in autophagy, the expression of autophagy proteins (raptor, rictor and LC3II/I) was further examined in the liver, as shown in

**Figure 5**. The mRNA levels of raptor and rictor showed that raptor mRNA levels were significantly decreased in mice were treated with all three options compared to mice fed the Lieber-DeCarli ethanol diet. Moreover, a significant reduction in raptor mRNA levels was observed in mice treated with a combination of LGG-s and BMMSCs. In addition, rictor mRNA levels were the opposite of raptor mRNA levels. There was a significant increase in rictor mRNA in mice treated with a combination of LGG-s and BMMSCs compared to mice only fed the Lieber-DeCarli ethanol diet (**Figure 5A**). The protein levels of raptor and rictor showed the same trends as observed at the mRNA levels (**Figure 5B**). mTOR is a complex with two forms: mTORC1 and mTORC2. The Raptor and Rictor proteins represent the distinctive components of these two forms, respectively (28). Furthermore, LC3II protein is a marker of autophagosome. The ratio of LC3II to LC3I can reflect the relative activity of autophagy. Their expression level was examined, as shown in **Figure 5B**. Although there was an increase in the LC3II/LC3I ratio in mice fed the Lieber-DeCarli ethanol diet compared to mice fed the normal control diet, there was no statistically significant difference among the treated groups except for the group of mice treated with the combination of LGG-s and BMMSCs, indicating an effect of the combination of LGG-s and BMMSC treatment on autophagy.

*Combined therapy regulates immune cells*

Since our previous investigation revealed that BMMSCs play an important role in immune reg-
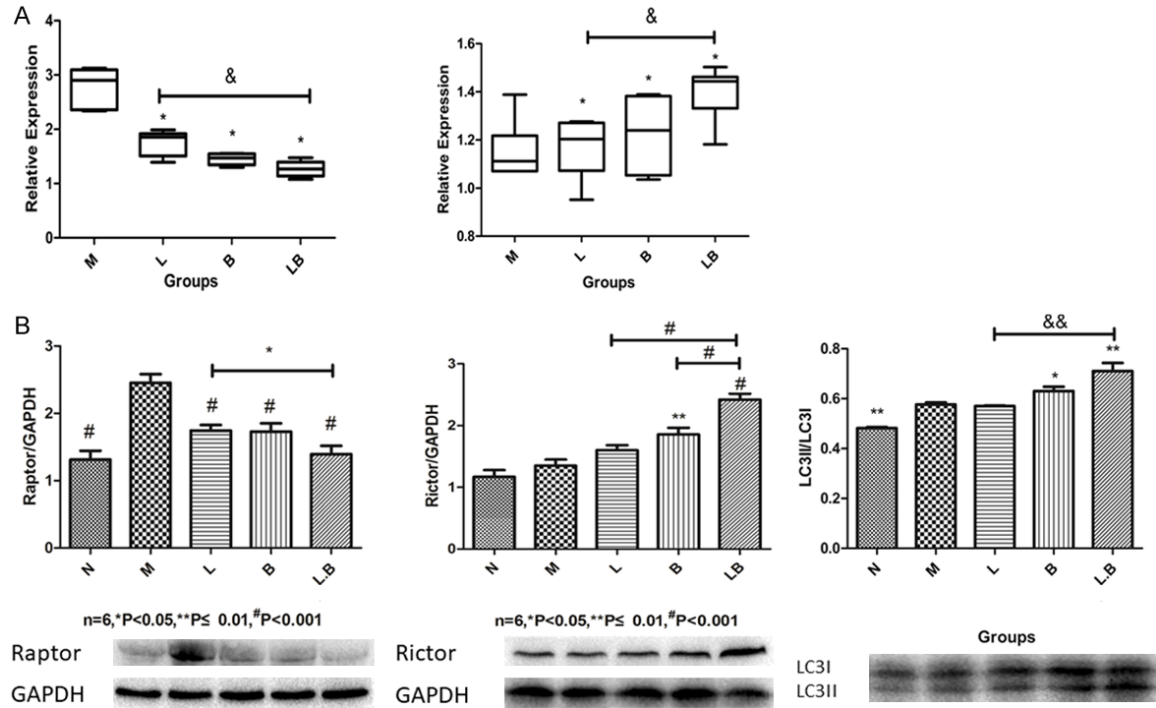
**Figure 5.** Expression of autophagy proteins - raptor, rictor and LC3II/LC3I in the livers from different groups. A. Shows the mRNA levels of raptor and rictor with raptor on the left and rictor on the right. B. Displays the protein levels of raptor, rictor and LC3II/LC3I; the upper panels are the histograms of the Western blot, and the lower panels are the typical pictures of the Western blots. Data are presented as the mean ± SEM from six mice in each group. *Represents P<0.05, **represents P<0.01, #represents P<0.001 vs group M. & and &&represents P<0.05 and P<0.01 between any 2 groups below the line.

ulation and the treatment of liver disease, the presence of NKB and TFH cells was investigated, as shown in **Figure 6**. The flow cytometry profile of NKB cells shown in **Figure 6A** reveals a significant increase in NKB cells in the spleens of mice fed the Lieber-DeCarli ethanol diet alone. However, treatment with all three options reduced the number of NKB cells in the spleen, with the most significant reduction observed in mice treated with the combination of LGG-s and BMMSCs. The flow cytometry profile of TFH cells is shown in **Figure 6B**, with similar changes in TFH T cell numbers in the different groups.

**Discussion**

In our previous publications, we investigated the role of bone marrow mesenchymal stem cells in the alleviation of inflammation in mice with acute liver injury and autoimmune hepatitis [33, 34]. Moreover, we investigated the therapeutic activity of LGG-s in acute alcoholic liver disease in mice [11]. However, whether the combination of LGG-s and BMMSCs affects

alcoholic liver disease remains unclear. Therefore, we designed an experiment to examine the therapeutic effects of a combination of LGG-s and BMMSCs on the attenuation of chronic-binge alcohol-induced liver injury. We examined inflammation, autophagy and immunomodulatory cell balance in mice.

The pathogenesis of alcoholic liver disease has been extensively investigated, but there is still no effective treatment for this disease. Since alcoholic liver disease, especially alcoholic steatohepatitis (ASH), involves several aspects of cellular and molecular biology, a single treatment will not completely heal alcohol-induced liver damage. In the liver, ASH shows both inflammation and autophagy effects, which are mediated by either the PI3K/NF-kB or PI3K/mTOR signaling pathways. It has been shown that the NF-kB signaling pathway is a major intracellular signaling pathway that induces the release of inflammatory cytokines, such as tumor necrosis factor-alpha (TNF-α) [5, 36]. The Lieber-DeCarli model of alcoholic liver injury is
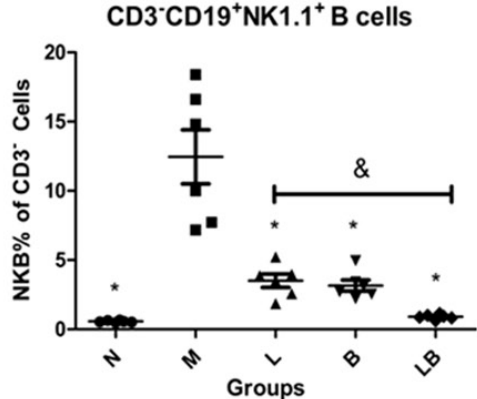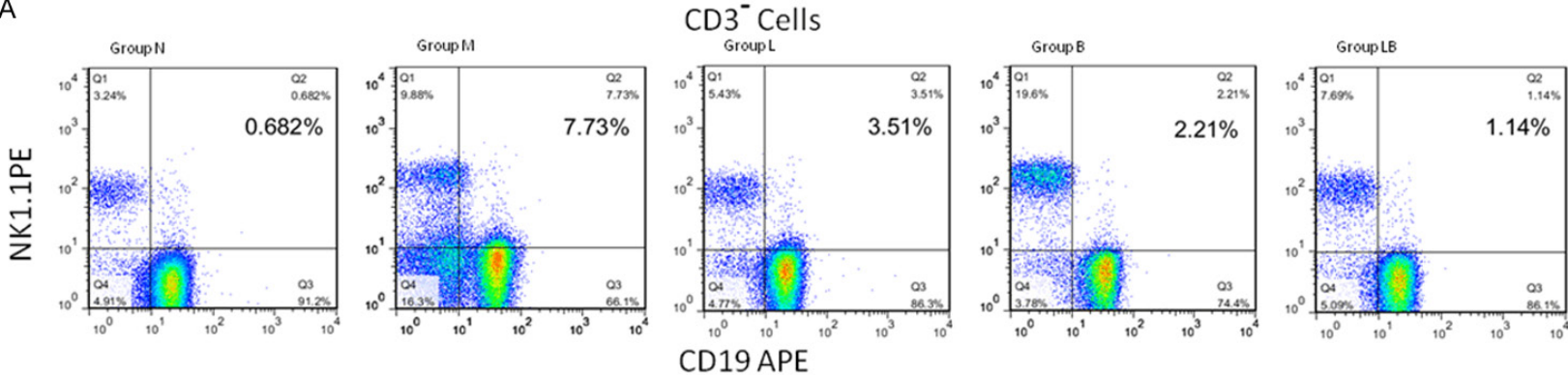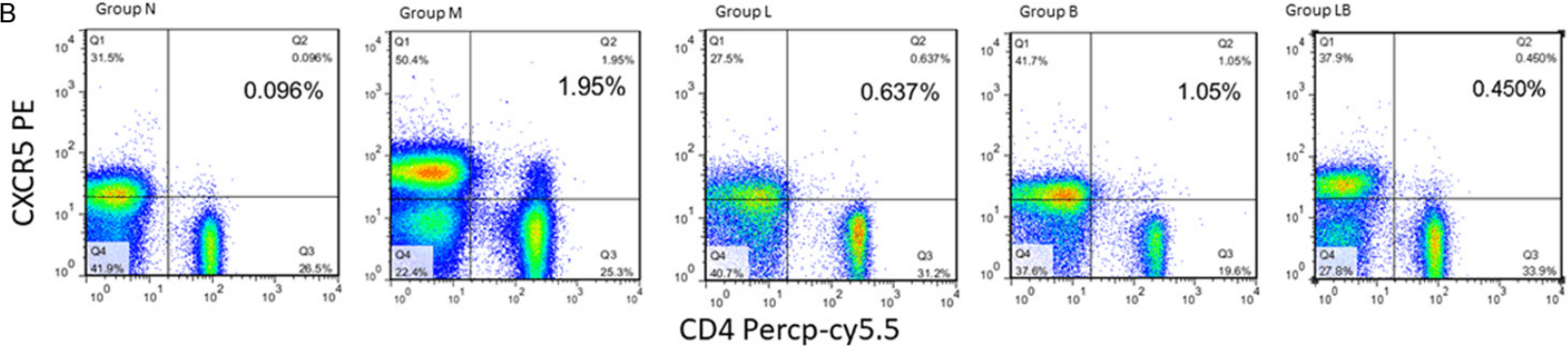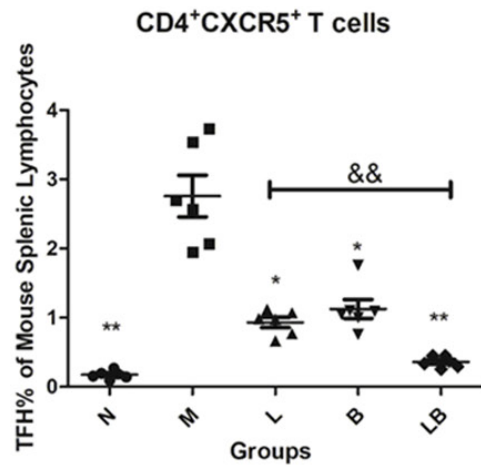
**Figure 6.** Flow cytometry analyses of NKB cells and TFH cells in the spleens from different groups. (A) Shows the NKB cell profile in the five experimental groups, and (B) displays the TFH cell profile in different groups. NKB cells in total B cells and TFH cells in total lymphocytes are shown as dot graphs in (A and B), respectively. Data are presented as the mean ± SEM from six mice in each group. *Represents $P<0.05$, **represents $P<0.01$ vs group M. & and &&represents $P<0.05$ and $P<0.01$ between any 2 groups below the line.

a good model to investigate inflammation of the liver. In this model, normal alcohol intake is simulated while providing sufficient daily calorie intake for the mice [35]. The results of body weight, serum ALT, AST, HE and oil red O staining analyses showed that the model was successfully established in our study. In addition, NF-kB signaling was activated in the model mice. With the three treatment options, we observed that with reduced NF-kB signaling, there was a decrease in liver injury. The activation of NF-kB signaling occurs through its phosphorylation, and the phosphorylation level reflects the degree of inflammation in the tissue [5, 36]. In our experiments, the activity of NF-kB in alcoholic mice was increased, whereas it was decreased in mice treated with the combination of LGG-s and BMMSCs. This result indicates that the combination of LGG-s and BMMSCs could inhibit NF-kB phosphorylation and reduce inflammation.

Autophagy is another pathological event in this model, as there was an increased level of LC3II/LC3I and activation of the mTOR signaling pathway in alcoholic mice. The signaling pathway of mTOR is associated with autophagy and innate immune regulation [24]. In this experiment, we found that the autophagy marker protein LC3II was elevated in alcoholic mice, which is consistent with the activation of autophagy. mTOR signaling is involved in both mTORC1 and mTORC2, which mediate either increased or decreased autophagy in cells [37, 38]. Although we observed that mTOR phosphorylation was reduced in mice treated with both LGG-s and BMMSCs and that LC3II level was also reduced, there was a low level of mTOR activity and low LC3II level in control mice. The differences between control mice and treated mice could be due to the ratio of mTORC1 to mTORC2 in the cells. The mTORC1 and mTORC2 signaling pathways involve raptor and rictor, respectively [39]. Although the phosphorylation of mTOR was decreased in mice treated with both LGG-s and BMMSCs, the level of mTORC2-associated rictor was elevated, which is different from that in the control mice. Therefore, although mTORC1 accounts for most of the mTOR complex, the role of mTORC2 is not negligible. It is the change in the proportion of the mTOR complex that regulates autophagy. We believe that the appropriate activation of autophagy alleviates liver damage in mice treated with both LGG-s and BMMSCs.

Our previous experiments showed that the treatment of LGG-s could affect the ratio of TH17 to Treg cells in mice, and the change in the proportion of these lymphocyte populations could improve the immune status of mice and thus protect the liver of mice with alcoholic hepatitis [11]. TFH cells are a subpopulation of T regulatory cells and are regulated by Treg cells and the mTOR signaling pathway. The activation of the mTOR pathway can promote TFH cell maturation and differentiation, and different components of mTOR complexes can regulate TFH cells differently. For example, raptor/mTORC1 mainly promotes CD4 T cell proliferation, which is necessary for TFH differentiation, while rictor/mTORC2 promotes Akt activation through TCF1 expression, which regulates TFH differentiation without severely affecting T cell proliferation [24-27]. Mature TFH cells are involved in innate immunity and humoral immunity [24-27]. However, few studies have been conducted on TFH cells in mice with alcoholic hepatitis, and there have been no investigations about the effect of interventions with probiotics and bone marrow mesenchymal stem cells on TFH cells in alcoholic liver disease. In this experiment, the proportion of TFH cells increased in mice with alcoholic hepatitis and decreased after treatment with LGG-s, BMMSCs or the combination of LGG-s and BMMSCs. Our findings reveal that inflammation in alcoholic hepatitis is closely associated with lymphocyte subsets, and the mTOR signaling pathway also plays a key role. Another type of lymphocyte, NKB cells, are a type of B cell with functions similar to those of helper T cells. NKB cells play an important role in infectious disease through the excretion of several cytokines. Our findings also found increases in the NKB cell population in alcoholic mice, and these populations decreased in response to treatment with LGG-s, BMMSCs and the combination of LGG-s and BMMSCs. These findings are consistent with the role of NKB cells in inflammation. In general, our findings reveal that in addition to playing a role in bacterial infections, TFH and NKB cells also play an influential role in diseases such as alcoholic hepatitis. These findings suggest that in alcoholic liver disease, the balance of the overall lymphocyte ratio is critical and therapeutic effect of BMMSCs and LGG-s it is mediated by this ratio. Moreover, these findings also suggest that mTOR signaling may also be involved in the reg-

ulation of the function and quantity of NKB cells through mTORC1 and mTORC2 mechanisms.

There are limitations to the current study. First, we did not directly verify that the BMMSC and LGG-s combination therapy regulates NF-kB and mTOR by acting on PI3K. Second, we cannot confirm whether our combination therapy acts directly on NKB cells or ultimately through the mTOR signaling pathway or both. Third, we did not directly analyze the effect of the changes in the ratio of TFH cells to NKB cells on the liver.

In summary, our study demonstrates that the LGG-s and BMMSC combination therapy can more effectively alleviate liver injury in alcoholic hepatitis than the individual therapies. The enhanced effect of the combination therapy may be related to its regulation of inflammation and autophagy through the NF-kB and mTOR signaling pathways. Moreover, the combination of LGG-s and BMMSCs in the treatment of alcoholic liver injury may also be related to the regulation of the balance between NKB and TFH cells.

## Disclosure of conflict of interest

None.

**Address correspondence to:** Drs. Yong-Ping Chen, Xiao-Dong Wang and Lan-Man Xu, Department of Infectious Diseases, The First Affiliated Hospital of Wenzhou Medical University, Hepatology Institute of Wenzhou Medical University, Wenzhou Key Laboratory of Hepatology, Wenzhou 325000, Zhejiang, China. E-mail: did@wzhospital.cn (YPC); xdwang0001@163.com (XDW); xulanman@163.com (LMX)

## References

[1] O'Shea RS, Dasarathy S, McCullough AJ; Practice Guideline Committee of the American Association for the Study of Liver Diseases; Practice Parameters Committee of the American College of Gastroenterology. Alcoholic liver disease. Hepatology 2010; 51: 307-328.

[2] Forner A, Llovet JM and Bruix J. Hepatocellular carcinoma. Lancet 2012; 379: 1245-1255.

[3] Carazo A, Leon J, Casado J, Gila A, Delgado S, Martin A, Sanjuan L, Caballero T, Munoz JA, Quiles R, Ruiz-Extremera A, Alcazar LM and Salmeron J. Hepatic expression of adiponectin receptors increases with non-alcoholic fatty liver disease progression in morbid obesity in correlation with glutathione peroxidase 1. Obes Surg 2011; 21: 492-500.

[4] Ma Z, Chu L, Liu H, Li J, Zhang Y, Liu W, Dai J, Yi J and Gao Y. Paeoniflorin alleviates non-alcoholic steatohepatitis in rats: Involvement with the ROCK/NF-kappaB pathway. Int Immunopharmacol 2016; 38: 377-384.

[5] Tian Y, Ma J, Wang W, Zhang L, Xu J, Wang K and Li D. Resveratrol supplement inhibited the NF-kappaB inflammation pathway through activating AMPKalpha-SIRT1 pathway in mice with fatty liver. Mol Cell Biochem 2016; 422: 75-84.

[6] Tsukamoto H. Metabolic reprogramming and cell fate regulation in alcoholic liver disease. Pancreatology 2015; 15 Suppl: S61-65.

[7] Gual P, Gilgenkrantz H and Lotersztajn S. Autophagy in chronic liver diseases: the two faces of Janus. Am J Physiol Cell Physiol 2017; 312: C263-C273.

[8] Liu C, Liao JZ and Li PY. Traditional Chinese herbal extracts inducing autophagy as a novel approach in therapy of nonalcoholic fatty liver disease. World J Gastroenterol 2017; 23: 1964-1973.

[9] Sinha RA and Yen PM. Thyroid hormone-mediated autophagy and mitochondrial turnover in NAFLD. Cell Biosci 2016; 6: 46.

[10] Ueno T and Komatsu M. Autophagy in the liver: functions in health and disease. Nat Rev Gastroenterol Hepatol 2017; 14: 170-184.

[11] Chen RC, Xu LM, Du SJ, Huang SS, Wu H, Dong JJ, Huang JR, Wang XD, Feng WK and Chen YP. Lactobacillus rhamnosus GG supernatant promotes intestinal barrier function, balances Treg and TH17 cells and ameliorates hepatic

injury in a mouse model of chronic-binge alcohol feeding. Toxicol Lett 2016; 241: 103-110.

[12] Guo F, Zou Y and Zheng Y. Moracin M inhibits lipopolysaccharide-induced inflammatory responses in nucleus pulposus cells via regulating PI3K/Akt/mTOR phosphorylation. Int Immunopharmacol 2018; 58: 80-86.

[13] Lei J, Zhao L, Zhang Y, Wu Y and Liu Y. High glucose-induced podocyte injury involves activation of mammalian target of rapamycin (mTOR)-induced endoplasmic reticulum (ER) stress. Cell Physiol Biochem 2018; 45: 2431-2443.

[14] Lee DK, Kim JH, Kim J, Choi S, Park M, Park W, Kim S, Lee KS, Kim T, Jung J, Choi YK, Ha KS, Won MH, Billiar TR, Kwon YG and Kim YM. REDD-1 aggravates endotoxin-induced inflammation via atypical NF-kappaB activation. FASEB J 2018; 32: 4585-4599.

[15] Wang B, Zheng SS, Zhou TY, Nie CH and Wan DL. Bigelovin, a sesquiterpene lactone, suppresses tumor growth through inducing apoptosis and autophagy via the inhibition of mTOR pathway regulated by ROS generation in liver cancer. Biochem Biophys Res Commun 2018; 499: 156-163.

[16] Czaja AJ. Current advances in the treatment of autoimmune hepatitis. Gastroenterol Hepatol (N Y) 2006; 2: 107-110.

[17] Than NN, Jeffery HC and Oo YH. Autoimmune hepatitis: progress from global immunosuppression to personalised regulatory T cell therapy. Can J Gastroenterol Hepatol 2016; 2016: 7181685.

[18] Manns MP, Jaeckel E and Taubert R. Budesonide in autoimmune hepatitis: the right drug at the right time for the right patient. Clin Gastroenterol Hepatol 2018; 16: 186-189.

[19] Hang P, Zhao J, Su Z, Sun H, Chen T, Zhao L and Du Z. Choline inhibits ischemia-reperfusion-induced cardiomyocyte autophagy in rat myocardium by activating Akt/mTOR signaling. Cell Physiol Biochem 2018; 45: 2136-2144.

[20] Eskelinen EL, Reggiori F, Baba M, Kovacs AL and Seglen PO. Seeing is believing: the impact of electron microscopy on autophagy research. Autophagy 2011; 7: 935-956.

[21] Naufel AO, Aguiar MCF, Madeira FM and Abreu LG. Treg and Th17 cells in inflammatory periapical disease: a systematic review. Braz Oral Res 2017; 31: e103.

[22] Miedema JR, Kaiser Y, Broos CE, Wijsenbeek MS, Grunewald J and Kool M. Th17-lineage cells in pulmonary sarcoidosis and Lofgren's syndrome: Friend or foe? J Autoimmun 2018; 87: 82-96.

[23] Wang S, Xia P, Chen Y, Huang G, Xiong Z, Liu J, Li C, Ye B, Du Y and Fan Z. Natural killer-like B cells prime innate lymphocytes against microbial infection. Immunity 2016; 45: 131-144.

[24] Zeng H, Cohen S, Guy C, Shrestha S, Neale G, Brown SA, Cloer C, Kishton RJ, Gao X, Youngblood B, Do M, Li MO, Locasale JW, Rathmell JC and Chi H. mTORC1 and mTORC2 kinase signaling and glucose metabolism drive follicular helper T cell differentiation. Immunity 2016; 45: 540-554.

[25] Yu D, Batten M, Mackay CR and King C. Lineage specification and heterogeneity of T follicular helper cells. Curr Opin Immunol 2009; 21: 619-625.

[26] Yang J, Lin X, Pan Y, Wang J, Chen P, Huang H, Xue HH, Gao J and Zhong XP. Critical roles of mTOR Complex 1 and 2 for T follicular helper cell differentiation and germinal center responses. Elife 2016; 5.

[27] Essig K, Hu D, Guimaraes JC, Alterauge D, Edelmann S, Raj T, Kranich J, Behrens G, Heiseke A, Floess S, Klein J, Maiser A, Marschall S, Hrabe de Angelis M, Leonhardt H, Calkhoven CF, Noessner E, Brocker T, Huehn J, Krug AB, Zavolan M, Baumjohann D and Heissmeyer V. Roquin suppresses the PI3K-mTOR signaling pathway to inhibit T helper cell differentiation and conversion of treg to Tfr cells. Immunity 2017; 47: 1067-1082, e12.

[28] Cassard AM and Ciocan D. Microbiota, a key player in alcoholic liver disease. Clin Mol Hepatol 2018; 24: 100-107.

[29] Miura K and Ohnishi H. Role of gut microbiota and Toll-like receptors in nonalcoholic fatty liver disease. World J Gastroenterol 2014; 20: 7381-7391.

[30] Bibbo S, Ianiro G, Dore MP, Simonelli C, Newton EE, Cammarota G. Gut microbiota as a driver of inflammation in nonalcoholic fatty liver disease. Mediators Inflamm 2018; 2018: 9321643.

[31] Chiu CC, Ching YH, Li YP, Liu JY, Huang YT, Huang YW, Yang SS, Huang WC, Chuang HL. Nonalcoholic fatty liver disease is exacerbated in high-fat diet-fed gnotobiotic mice by colonization with the gut microbiota from patients with nonalcoholic steatohepatitis. Nutrients 2017; 9.

[32] Chen YT, Lin YC, Lin JS, Yang NS and Chen MJ. Sugary kefir strain lactobacillus mali APS1 ameliorated hepatic steatosis by regulation of SIRT-1/Nrf-2 and gut microbiota in rats. Mol Nutr Food Res 2018; 62: e1700903.

[33] Chen Y, Chen S, Liu LY, Zou ZL, Cai YJ, Wang JG, Chen B, Xu LM, Lin Z, Wang XD and Chen YP. Mesenchymal stem cells ameliorate experimental autoimmune hepatitis by activation of the programmed death 1 pathway. Immunol Lett 2014; 162: 222-228.

[34] Cai Y, Zou Z, Liu L, Chen S, Chen Y, Lin Z, Shi K, Xu L and Chen Y. Bone marrow-derived mesenchymal stem cells inhibits hepatocyte apoptosis after acute liver injury. Int J Clin Exp Pathol 2015; 8: 107-116.

[35] Guo F, Zheng K, Benede-Ubieto R, Cubero FJ and Nevzorova YA. The Lieber-De Carli diet - a flagship model for experimental Alcoholic Liver Disease (ALD). Alcohol Clin Exp Res 2018.

[36] Russo MA, Sansone L, Carnevale I, Limana F, Runci A, Polletta L, Perrone GA, De Santis E and Tafani M. One special question to start with: Can HIF/NFkB be a target in inflammation? Endocr Metab Immune Disord Drug Targets 2015; 15: 171-185.

[37] Dhar SK, Bakthavatchalu V, Dhar B, Chen J, Tadahide I, Zhu H, Gao T and St Clair DK. DNA polymerase gamma (Polgamma) deficiency triggers a selective mTORC2 prosurvival autophagy response via mitochondria-mediated ROS signaling. Oncogene 2018; 37: 6225-6242.

[38] Ito M, Yurube T, Kakutani K, Maeno K, Takada T, Terashima Y, Kakiuchi Y, Takeoka Y, Miyazaki S, Kuroda R and Nishida K. Selective interference of mTORC1/RAPTOR protects against human disc cellular apoptosis, senescence, and extracellular matrix catabolism with Akt and autophagy induction. Osteoarthritis Cartilage 2017; 25: 2134-2146.

[39] Meade N, Furey C, Li H, Verma R, Chai Q, Rollins MG, DiGiuseppe S, Naghavi MH and Walsh D. Poxviruses evade cytosolic sensing through disruption of an mTORC1-mTORC2 regulatory circuit. Cell 2018; 174: 1143-1157.